scientific reports

Check for updates

OPEN

GelMA encapsulating BMSCs-exosomes combined with interference screw or suture anchor promotes tendon-bone healing in a rabbit model

Mingyang Gao[1,2,3], Piqian Zhao[2,3], Junhui Xing[2], Zhuolin Wang[1], Yingjie Xu[2], Yurong Yan[1], Hongtao Zhang[2]✉ & Jing Qu[1]✉

The tendon-bone junction (TBJ), a critical transitional zone where tendons and bones connect, is particularly prone to injury due to the forces from muscle contractions and skeletal movements. Once tendon-bone injuries occur, the complex original tissue structure is difficult to restore, increasing the risk of re-tear. In this study, we initially established a rabbit model of tendon-bone injury and treated it using either interference screw or suture anchor. Biomechanical testing demonstrated the maximum tension and strength of TBJ with interference screw fixation were superior. However, histologic and immunohistochemical results showed more tissue regeneration and expression of cartilage markers at the site of injury with suture anchor fixation. Moreover, Gelatin Methacryloyl encapsulated with exosomes from mesenchymal stem cell (GelMA-exosomes) were prepared, showing a consistent and stable exosome release characteristic. The combined application of GelMA-exosomes with either interference screws or suture anchors further enhanced the healing of tendon-bone injuries, which may be achieved by promoting cellular proliferation as well as regulating the decreased expression of local pro-inflammatory factors IL-1β, IL-6 and TNF-α and increased expression of anti-inflammatory factors IL-10 and TGF-β. This provides a viable therapeutic strategy to enhance tendon-bone healing.

Keywords Mesenchymal stem cell, Exosomes, Gelatin methacryloyl, Tendon-bone healing

The tendon-bone junction (TBJ), where the soft tissue tendon attaches to the bone, is a site with a complex structure. The TBJ can be divided into four parts: tendon tissue, uncalcified fibrocartilage tissue, calcified fibrocartilage tissue, and bone[1–3]. The tendon tissue is mainly composed of type I collagen. The uncalcified fibrocartilage is made up of mainly type II and III collagen and a small amount of type I and X collagen. Calcified fibrocartilage is mainly composed of type II and X collagen. The bone tissue mainly consists of type I collagen and apatite. The fibrocartilage tissue is mechanically weaker than the tendon and bone tissue and thus is prone to injury[4–8]. Tissue repair is usually dominated by fibrous scar tissue after injury. The disturbed scar tissue is mainly composed of type III collagen, which is much less mechanically robust than normal tissue, resulting in a high rate of postoperative retears. Some studies have reported that retear rates are as high as 20–94% after tendon-bone reconstruction[9]. Therefore, tendon-bone injury repair is a notable challenge in orthopedics and sports medicine.

Bone marrow-derived mesenchymal stem cells (BMSCs) are adult stem cells derived from the mesoderm which can self-regenerate, with multidirectional differentiation and immunomodulatory potential[10–12]. Numerous studies have applied BMSCs to the repair of TBJ injuries[13–16]. BMSCs have been demonstrated to promote the regeneration of fibrocartilage and tendon tissue in the early stages of injury, which enhances the biomechanics of the tendon-bone healing site[17]. However, the implantation of BMSCs may also result in teratomas or ectopic bone formation in the tendon[18]. Recent studies revealed extracellular vesicles from BMSCs

[1]Department of Cell Biology, School of Biology and Basic of Medical Science, Medical College of Soochow University, Suzhou 215123, China. [2]Department of Orthopedics, the First Affiliated Hospital of Soochow University, Soochow University, Suzhou, Jiangsu, China. [3]These authors contributed equally: Mingyang Gao and Piqian Zhao. ✉email: htzhangsz@163.com; qujing@suda.edu.cn

can promote tissue repair through a paracrine pathway, indicating that it could be used as an alternative treatment for transplantation of BMSCs[19].

Exosomes are a type of extracellular vesicle that almost all types of cells can secrete. They transmit mRNA, miRNA, proteins, and other substances secreted by the donor cell to the recipient cell, participating in intercellular material communication and tissue repair[20–22]. The study of Han et al. found that BMSCs-derived exosomes (BMSCs-exosomes) could upregulate the expression of tendon and cartilage-related factors to treat rotator cuff injuries[23]. There are also some studies have found that BMSCs-exosomes were able to reduce inflammation and increase cartilage factor expression around the injured tissue[9,24,25]. However, few studies have explored the therapeutic effect of interference screw or suture anchor incorporated with BMSCs-exosomes in TBJ.

In addition, BMSCs-exosomes injected into the injury site as an aqueous solution are not conducive to its prolonged retention and make it difficult to fully perform its biological function. The studies of Chen and Ju et al. reported GelMA hydrogel-loaded exosomes for the treatment of tissue damage[26,27]. GelMA hydrogels have good biocompatibility and loose and porous structural properties, which can be used as a carrier for exosomes to facilitate their prolonged retention and stable release at specific sites[27]. Therefore, our study used GelMA hydrogel-loaded exosomes and implanted it into the TBJ to investigate its repair effect.

Interference screws and suture anchors are commonly used for tendon-to-bone fixation in clinical surgery[28–31]. The interference screw places the tendon in the bone tunnel while the suture anchor implants the anchor into the bone to form the fixation[32]. The suture connected to the anchor stitches the tendon, refixing the tendon to the bone surface[33]. However, there are few studies comparing the therapeutic effects of the two methods at the TBJ.

This study aimed to investigate the therapeutic effect of GelMA-exosomes at the TBJ during interference screw or suture anchor fixation and compare the two fixation methods. We hypothesized that GelMA-exosomes may promote tendon-bone healing through its biological activity. Meanwhile, due to the large contact area between tendon and bone during interference screw fixation, we hypothesized that interference screw fixation would be more stable.

Results

Multi-lineage differentiation and identification of rabbit BMSCs

In this study, rabbit BMSCs were isolated and cultured by the whole bone marrow apposition method. Primary cultures showed oval or spherical colony-like adherent growth (Fig. 1A). The BMSCs were gradually and evenly distributed after the first generation, with most cells growing in a swirling pattern and some cells showing a spindle-like morphology (Fig. 1B). After the third generation, a uniform and regular distribution of cells can be observed growing in a long shuttle pattern attached to the wall (Fig. 1C). Flow cytometry showed high expression of CD44 and negative expression of CD34 and CD45 [34]. The results of the induced differentiation showed that the osteogenic-differentiated cells were stained with alizarin red and found to be orange in color and aggregated into calcareous nodules, indicating that the rabbit BMSCs were capable of osteogenic differentiation (Fig. 1D). Chondrogenic differentiation-induced cells were stained with Alisin Blue, and reticulate blue chondrocytes were found, indicating that rabbit BMSCs are capable of chondrogenic differentiation (Fig. 1E). Adipogenic-induced differentiation of cells was stained with Oil Red O, where the lipid droplets stained red, indicating that rabbit BMSCs are capable of adipogenic differentiation (Fig. 1F).

BMSCs-exosomes characterization

The exosomes were photographed by TEM, and their typical teacup-like vesicle structure could be observed (Fig. 1G). NTA examined the particle size of the exosomes and found that the extracted particles were concentrated around 100–200 nm in size (Fig. 1H). Western Blot assay detected signature proteins on the surface of exosomes and found positive expression of CD9, CD81, TSG101 and negative expression of Calnexin in exosomes (Fig. 1I).

Distribution and release dynamics of BMSCs-exosomes in GelMA Scaffolds

The scaffolds were prepared with two different densities of 5% GelMA-30 and 5% GelMA-60. The pictures were taken using scanning electron microscopy and analyzed using ImageJ software. The results revealed that GelMA-30 had larger pores and overall relaxation, while GelMA-60 had higher porosity (Fig. 2A). In order to ensure the loading efficiency of BMSCs-exosomes, we chose GelMA-60 with higher porosity for subsequent studies. The PKH26 was used to stain BMSCs-exosomes and mixed with equal amounts of PBS and GelMA, respectively. 2D and 3D photographs were taken using confocal microscopy to observe their distribution in the two media. It was found that after staining with PKH26 BMSCs-exosomes was in the form of red granules, uniformly distributed in both PBS and GelMA (Fig. 2B). No local aggregation of BMSCs-exosomes was observed in GelMA, satisfying the requirements for transplantation.

PKH26-labelled BMSCs-exosomes was used to assess the release profile of GelMA-exosomes. GelMA-exosomes were placed in PBS at room temperature and the supernatant was collected every 24 h. Seven days later, fluorescence quantification was performed using an enzyme marker. The results showed that the daily release of BMSCs-exosomes from GelMA-exosomes decreased gradually over time, with the release of BMSCs-exosomes up to approximately 80% of the initial amount at one week (Fig. 2C). This indicates that GelMA-exosomes could be consistently and steadily released around the injured tissue.

BMSCs-exosomes inhibited inflammatory factors and promoted cells proliferation

QRT-PCR experiments were performed to detect the expression of inflammatory factors and tissue repair-related factors in the injured tissues. The results showed that the expression of IL-1β, IL-6, and TNF-α in the GelMA-exosomes group was significantly lower than that in the Control and GelMA groups ($P<0.05$), while the expression of IL-10 and TGF-β was higher than that in the control and GelMA groups ($P<0.05$) (Fig. 4A).

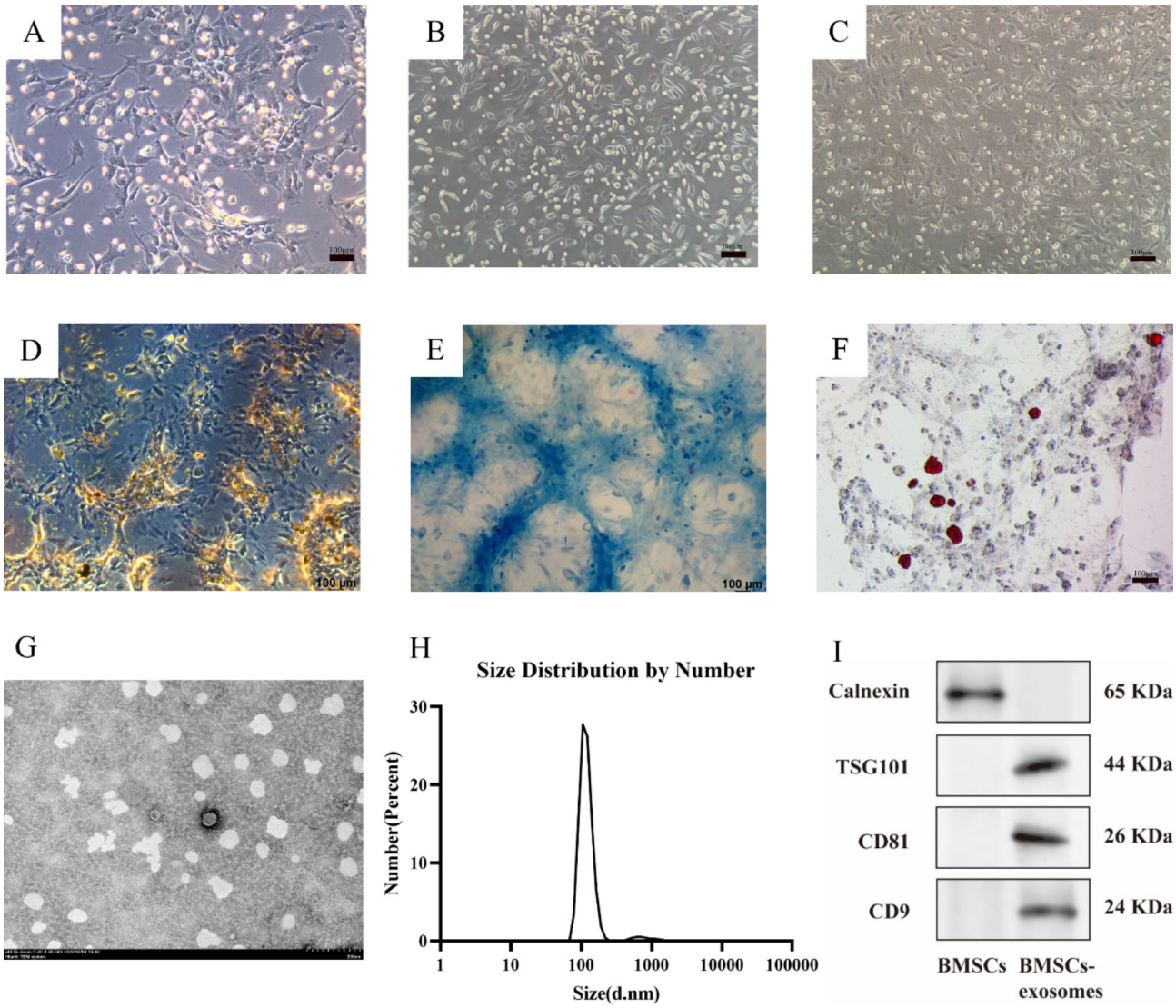

Fig. 1. Morphological Observation of BMSCs, identification of BMSCs, and BMSCs-exosomes Characterization. (**A**) P0 generation showed granule-like aggregation. (**B**) P1 generation showed short spindle-shaped apposition. (**C**) P3 generation showed spindle-shaped appressed growth. (**D**) Osteogenic differentiation of rabbit BMSCs showed yellow calcium nodules. (**E**) Chondrogenic differentiation of rabbit BMSCs showed blue reticular chondrocytes. (**F**) Adipogenic differentiation of rabbit BMSCs showed red lipid droplets. Scale bar: 100 μm. (**G**) TEM showed a teacup-like vesicle structure of BMSCs-exosomes. Scale bar: 200 μm. (**H**) NTA showed that the particle size of BMSCs-exosomes was clustered at 100–200 nm. (**I**) Western Blot results showed high expression of CD9, CD81, TSG101 and low expression of Calnexin.

Moreover, no significant differences in the expression of inflammatory factors were observed between the suture anchor and interference screw groups. These results suggest that BMSCs-exosomes could alleviate the inflammatory response in injured tissues at an early stage, whereas the choice of the fixation device has no significant effect on the local inflammatory response. Edu assay was performed to detect the early proliferation of cells in the injured tissue. The experiment was divided into two groups: the PBS and the BMSCs-exosomes groups. The results showed that more cells proliferated in the BMSCs-exosomes group than in the PBS group ($P < 0.05$) (Fig. 4C). BMSCs-exosomes stained with PKH26 red fluorescent dye were clustered around the nucleus (Fig. 4B), indicating that BMSCs-exosomes could promote cell proliferation.

Histological analysis of the TBJ

The HE and SO-FG staining results (Fig. 5A) showed that at the third week of interference screw fixation, the tendon-bone interface in the control group was clearly demarcated, and no new fibro chondrocytes were seen. In the GelMA group, new chondrocytes were seen in the bone and tendon tissues, but only a small number of new chondrocytes gathered at the tendon-bone interface. In the GelMA-exosomes group, new chondrocytes gathered at the tendon-bone interface, but the distribution was disorganized. In the sixth week, the boundary between the tendon-bone interface still existed in the control group, the tendon-bone gap was narrowed, and

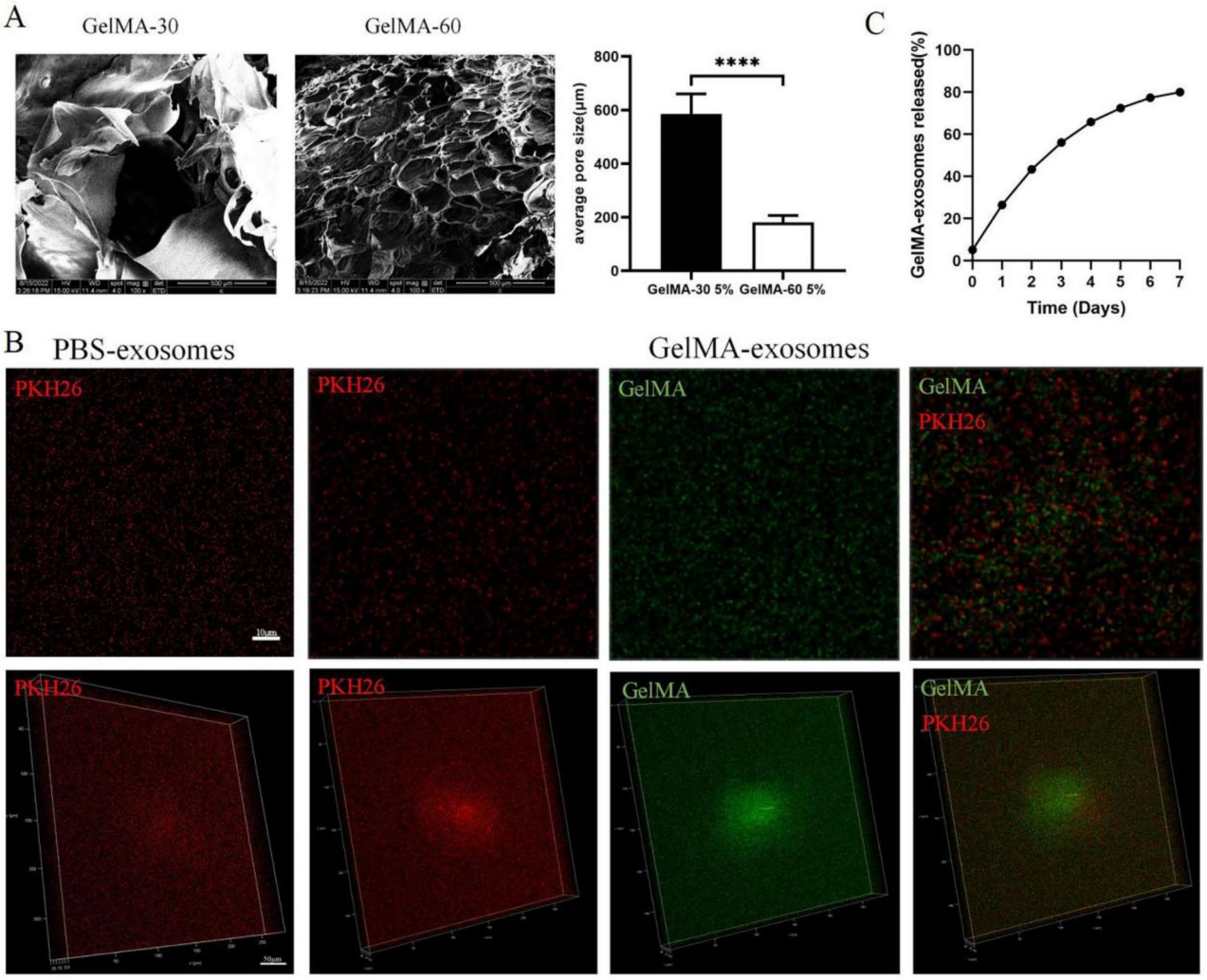

Fig. 2. Distribution and release dynamics of BMSCs-Exosomes in GelMA. (**A**) Scanning electron microscopy images and quantitative pore size analysis of 5% GelMA-30 and 5% GelMA-60. (**B**) Distribution of BMSCs-exosomes in PBS and GelMA, BMSCs-exosomes (PKH26 red fluorescence staining), GelMA (green fluorescence). (**C**) Release curve of GelMA-exosomes during 7 days.

new chondrocytes were distributed at both ends of the interface with a uniform arrangement. New blood vessels grew into the tendon-bone interface in the GelMA group, and many chondrocytes gathered on the bone surface. The tendon-bone boundary was blurred in the GelMA-exosomes group, and chondrocytes gathered on the bone surface. The new tissue was evenly arranged and distributed.

The results (Fig. 5B) showed that at the third week of suture anchor fixation, the tendon-bone interface in the control group was clearly demarcated and no new chondrocytes were seen. In the GelMA group, few new chondrocytes were seen at both ends of the tendon-bone interface with local gaps in the tissue. The tendon-bone interface of the GelMA-exosomes group was found to be an aggregation of new chondrocytes with well-aligned new tissue. In the sixth week, the tendon-bone interface in the control group was blurred, with new chondrocytes aggregating on the bone surface, localized discontinuity of bone tissue, and poor tendon-bone integration. In the GelMA group, the tendon-bone demarcation was blurred, with localized cartilage-like migration structures and a disorganized arrangement of new chondrocytes and extracellular matrix. In the GelMA-exosomes group, new tissue fused with normal tissue and cartilage-like migration structures were seen at the tendon-bone interface, with good tendon-bone integration.

Immunohistochemical analysis of the TBJ

The Col II and Acan immunohistochemistry staining results (Fig. 6A) showed that at the third week of interference screw fixation, no positive expression of chondrocytes and cartilage matrix at the tendon-bone interface in the control group. In the GelMA group, Col II and Acan staining showed a small number of chondrocytes positively expressed. In the GelMA-exosomes group, Col II staining revealed new chondrocytes aggregated on the bone surface. Acan staining revealed brownish-yellow cartilage matrix secretion aggregated at the tendon-bone interface. In the sixth week, Col II and Acan staining in the control group showed that new chondrocytes and

cellular matrix gathered at the tendon-bone interface, with a clear demarcation between tendon and bone. In the GelMA group, Col II and Acan staining showed many new chondrocytes, but no fibrocartilage connection appeared at the tendon-bone interface. In the GelMA-exosomes group, Col II and Acan staining showed that new chondrocytes and extracellular matrix were well arranged and evenly distributed at the tendon-bone interface, with blurred tendon-bone demarcation and localized migrating structures.

The staining results at the time of suture anchor fixation were as follows (Fig. 6B). In the third week, Col II staining showed no new chondrocytes and extracellular matrix expression. Acan staining revealed a small amount of brownish cartilage matrix secretion in the tendon and bone tissue, and only a few new chondrocytes gathered at the tendon-bone interface in the control group. In the GelMA group, Col II and Acan staining showed clear tendon-bone demarcation, local gaps, and sparse distribution of new chondrocytes. In the GelMA group, Col II and Acan staining revealed a sparse distribution of new chondrocytes clustered at the tendon-bone interface. In the GelMA-exosomes group, Col II and Acan staining showed that new chondrocytes and extracellular matrix were distributed at both ends of the tendon-bone interface. The neoplastic tissue was disorganized, with clear tendon-bone demarcation with local gaps. In the sixth week, Col II and Acan staining in the control group showed many new chondrocytes and extracellular matrix gathered at the tendon-bone interface, but the new tissue was disorganized and poorly integrated with normal tissue. In the GelMA group, Col II and Acan staining revealed many new chondrocytes and extracellular matrix aggregates at the tendon-bone interface, with an orderly arrangement of new tissues and localized fibrocartilage migration structures. In the GelMA-exosomes group, Col II and Acan staining showed blurring of the tendon-bone interface demarcation line and the appearance of migrating structures. The new organization were well-arranged and evenly distributed. In order to compare the repair effect of the tendon-bone interface when the TBJ is fixed with interference screws and suture anchors, a quantitative analysis of the positive areas was performed using ImageJ for Col II and Acan immunohistochemical results (Fig. 6C–F). The results revealed that the positive expression of new chondrocytes was greater in the GelMA-exosomes group than in the GelMA and Control groups ($P < 0.05$) both in interference screw fixation and suture anchor fixation. Therefore, adding GelMA-exosomes at the injury site could promote chondrocyte regeneration. The results also found that the expression of new cartilage at the TBJ was greater with suture anchor fixation than with interference screw fixation ($P < 0.05$).

Biomechanical testing

In order to measure the strength of the TBJ, biomechanical test was performed at six weeks postoperatively (Fig. 7). The results revealed that the maximum tension and strength of the GelMA-exosomes group were superior to those of the control and GelMA groups ($P < 0.05$) whether fixed with interference screw and suture anchor, indicating that the GelMA-exosomes was able to promote tissue healing at the TBJ and strengthen the tendon-bone connection. From the results we can also found that the maximum tension and strength of the TBJ with interference screw fixation were superior to those with suture anchor fixation ($P < 0.05$).

GelMA-exosomes promoted bone regeneration around bone tunnels

The specimens were scanned by Micro-CT and reconstructed as tomograms by NRecon Reconstruction software. 3D reconstruction was carried out by CTVox software. CTan software was used to analyze and measure the formation of new bone tissue around the tunnel. The black circle in (Fig. 8A) is a 4 mm diameter circular bone tunnel at the time of interference screw placement. No significant change in the upper cortical aperture of the bone tunnel was seen during interference screw fixation, which was related to the screw being in place. The filling of the screw inhibited the horizontal growth of the new bone into the bone tunnel. Quantification of relative bone volume or bone volume fraction (BV/TV), Trabecular Number (Tb. N), Trabecular Separation/Spacing (Tb. Sp), Trabecular Thickness (Tb. Th) of the upper bone cortex. The results showed that the BV/TV, Tb. N and Tb. Th values of bone in the GelMA-exosomes group were higher than those in control and GelMA groups at 3 and 6 weeks postoperatively ($P < 0.05$) while the Tb. Sp values of bone in the GelMA-exosomes group were lower than those in the Control and GelMA groups ($P < 0.05$). It is shown that GelMA-exosomes could promote the formation of new bone on the surface and reduces bone resorption during interference screw fixation.

The black circle in (Fig. 8B) is a 2 mm diameter circular bone tunnel at the time of a suture anchor placement. A notable reduction in the cortical aperture of the upper layer of the bone tunnel at week 6 compared to week 3 was seen with suture anchor fixation. This differed from an interference screw in that the suture anchor was implanted within the bone tissue. There was no anchor filling in the upper bone cortex, except sutures passing through. The horizontal growth of the new bone into the bone tunnel was not inhibited. The results of the quantitative analysis revealed that the values of BV/TV, Tb. N and Tb. Th of bone in the GelMA-exosomes group were higher than those of the control and GelMA groups with suture anchor fixation ($P < 0.05$), while the values of Tb. Sp of bone were lower than those of the control and GelMA groups ($P < 0.05$). It demonstrated that GelMA-exosomes could promote the formation of new mineralized bone on the surface with suture anchor fixation and promote the repair of bone on the surface of the tendon-bone interface.

Discussion

Tendon-bone injury repair is a challenge in orthopaedics and sports medicine due to the limited regenerative capacity of its original fibrocartilage structure. Some studies have reported that the process of tendon-bone healing undergoes three stages of inflammation, proliferation, and remodeling[35–37]. In the early stages of healing, an acute inflammatory response occurs in the injured area, with extensive infiltration of M1 macrophages. M1 macrophages secrete pro-inflammatory factors, including TNF-α, IL-1β, and IL-6, which have been shown to inhibit chondrogenic differentiation and cartilage matrix formation. In addition, the inadequate blood supply to the fibrocartilage itself leads to a problematic regeneration of the fibrocartilage layer at the tendon-bone interface,

which is eventually replaced by scar tissue consisting of Sharpey fibers, resulting in poor healing of the TBJ[38]. M2 macrophages can release anti-inflammatory factors, such as IL-10 and TGF-β. Some studies have demonstrated that TGF-β is a crucial regulator of chondrogenic differentiation and can promote the proliferation and repair of cartilage[39–41]. Thus, the reduction of tissue inflammation, the increase in tissue blood supply, and the promotion of chondrocyte regeneration are beneficial to TBJ healing. Recently, some progress has been made in using stem cell therapy to treat injuries at the tendon-bone interface. The most commonly used of these are BMSCs. BMSCs can proliferate and differentiate into target cells to replace the missing cells at the injury site. However, there are currently no uniform standards for the dose and frequency of stem cell therapy. Injections of stem cells may cause adverse risks, such as immune reactions and tumor formation, which hinder their further clinical application[42,43]. It has been shown that stem cell therapy is not limited to cell regeneration and differentiation but can also secrete large numbers of extracellular vesicles through paracrine action, which regulates the local environment around cells and participate in tissue repair and metabolism[44,45]. BMSCs-exosomes were able to regulate macrophage polarization, reduce inflammation and induce peripheral vessel formation at the end of the injury site. Our findings also revealed the ability of BMSCs-exosomes to inhibit the production of inflammatory factors and promote the formation of anti-inflammatory factors and cartilage growth factors at the injury site[9,24,46].

BMSCs-exosomes are often injected directly into the circulatory system or body cavity as an aqueous solution to promote tissue healing. However, it is difficult for BMSCs-exosomes in an aqueous solution to be retained in the injured area for an extended period, ultimately making it difficult for BMSCs-exosomes to function adequately[46–48]. In order to retain BMSCs-exosomes at the injury site for an extended period, GelMA hydrogel was used to encapsulate BMSCs-exosomes. GelMA hydrogel is a biocompatible and degradable biomaterial, and its inherent porous structure facilitates the storage of cytokines[49]. In this study, SEM was used to observe the microstructure of 5% GelMA-30 and 5% GelMA-60, which were found to have a porous multilayer structure. The distribution of BMSCs-exosomes in PBS and GelMA was photographed using confocal microscopy and found to be uniformly distributed in GelMA. In vitro, release experiments of GelMA-exosomes showed a slow release of BMSCs-exosomes over time in 7 days. The amount released on the seventh day was up to 80% of the initial amount. Our research have found that GelMA-exosomes could release stably and retain for a relatively long time, which were conducive to the full action of the exosomes and provide inspiration for the practical application of exosomes.

Interference screw and suture anchor are often used to attach the tendon to the bone surface in clinical surgery[31,50]. However, few studies have compared the repair of two fixation methods in the TBJ. The interference screw fixed the tendon to the bone surface by squeezing pressure between the screw and the bone tunnel. The local stress helps the tendon to make contact with the bone. However, the degree of damage to the bone and surrounding soft tissues during interference screw fixation is high and the strength of the screw fixation is influenced by several factors, including limb bone density, thread height, position, length, and gap size[31,51,52]. The suture anchor was embedded into the bone and the tendon was fixed to the bone surface by sutures on the anchor nail. The degree of damage to the bone and surrounding tissue with suture anchor fixation was minimal, but the local pressure of the sutures on the tendon-bone interface was weaker than with an interference screw. In this study, biomechanical experimental results revealed superior tendon-bone connection strength with interference screw fixation. This may be due to the contact area between the tendon and the bone being greater with interference screw fixation than with suture anchor fixation, or it may be that the squeeze force between the screw and the bone is greater than the fixation force of the suture. Histological and immunohistochemical staining results showed more tissue regeneration and cartilage tissue expression at the injury site with suture anchor fixation than with interference screw fixation. Although the early fixation strength of the TBJ with suture anchor was weaker than that with interference screw, more tissue regeneration and chondrocyte expression at the TBJ with suture anchor fixation than with interference screw fixation in terms of microstructure. This phenomenon may be because tendon and bone tissue are less damaged with suture anchor fixation, which is an advantage of suture anchor fixation compared to interference screw fixation.

Meanwhile, interference screw and suture anchor, as foreign bodies, implantation may cause a rejection reaction in the organism. Moreover, an early inflammatory reaction is detrimental to the healing of the tendon-bone union[53]. In our study, GelMA-exosomes was added after fixation of the TBJ with an interference screw or a suture anchor. The expression of IL-1β, IL-6, and TNF-α was significantly lower in the GelMA-exosomes group, while the expression of IL-10 and TGF-β was more than that in the negative control and GelMA groups. We also found more tissue regeneration and chondrocyte-like cell expression in the GelMA-exosomes group than other groups in histology. This phenomenon occurs in both interference screw and suture anchor fixation. In the biomechanical and Micro-CT experimental results, it was found that the strength of the tendon-bone connection and bone repair in the GelMA-exosomes group were better than those in the other two groups. BMSCs-exosomes could inhibit tissue inflammation at an early stage and promote the healing of the TBJ, providing a new idea for tendon-bone healing.

Conclusion

Our study found that tendon-bone connection was more stable with interference screw fixation, and the cartilage tissue regeneration and expression at the tendon-bone interface were greater with suture anchor fixation, which can be used as a reference for clinical procedure. The GelMA-exosomes prepared in this study were able to be released stably in vitro, which contributed to their full biological activity. Furthermore, our study found that GelMA-exosomes could intervene the early process of tendon-bone healing, inhibit inflammation, and promote the repair of TBJ, which may be used as a therapeutic option for tendon-bone healing. This study discusses the therapeutic efficacy of interference screw and suture anchor in the TBJ. The addition of GelMA-exosomes was

found to result in a faster and better repair in the TBJ, with a closer approximation to the structure of normal tissue.

Methods

Cell culture and characterization

New Zealand rabbits weighing approximately 0.4–0.5 kg (regardless of gander) were selected as the source of primary BMSCs. The ends of the epiphyses were cut, the middle bone marrow was then extracted and centrifuged at 1000 rpm for 5 min. The supernatant was removed, and 2 mL of L-DMEM (Gibco, USA) containing 10% fetal bovine serum (Gibco, USA) was added for resuspension. The cells were evenly divided into six-well plates and incubated at 37 °C in a 5% incubator. Suitable rabbit BMSCs were selected and made into single-cell suspensions. BMSCs were identified using flow cytometry with the cell surface markers Rabbit Anti-CD34/FITC (1:100, Bioss, China), Rabbit Anti-CD44/FITC (1:100, Bioss, China), and Rabbit Anti-CD45/FITC (1:100, Bioss, China). As described in the literature, suitable cells were selected for induction of chondrogenic, osteogenic, and adipogenic differentiation and identified by Alisin Blue (Sigma, USA), Alizarin Red (Sigma, USA), and Oil Red O (Sigma, USA) staining respectively after 21 days.

Exosomes preparation and identification

BMSCs cultured to P3 generation were transferred to 6-well plates, and cell supernatants were collected daily when the cell density grew to 80% (approximately 5×10^5 cells/well). BMSCs-exosomes in the supernatant were extracted according to the instructions of the VEX Exosome Isolation Reagent kit (Vazyme, China), and the concentration of exosomes was measured using the BCA protein quantification kit (Beyotime, China). The structure of the exosomes was observed using transmission electron microscopy (TEM; Titan, FEL, USA), the size distribution and concentration of the exosomes were determined by nanoparticle tracking characterization system (Zatasizer Nano ZS90, Malvern Panalytical), and the surface-specific proteins Calnexin (Bioss, China), CD9 (Bioss, China), CD81 (Bioss, China), and TSG101 (Bioss, China) were detected by Western Blot.

BMSCs-exosomes labeling

First, 500 µl BMSCs-exosomes (50 µg/ml) were resuspended in 0.5 ml Diluent C (Solarbio, China) and then mixed with 4 µl PKH26 (Solarbio, China). The solution was incubated at room temperature and avoided light for 5 min. Then, 2 ml of 0.5% BSA (Beyotime, China) was used to end the staining. The mixture was centrifuged at 10,0000 g for 70 min to remove the residual dye, followed by resuspension of the precipitate in 200 µl phosphate buffered saline (PBS).

GelMA preparation and pore size analysis

A 0.25% initiator standard solution (EFL, China) was prepared according to the kit instructions. 0.5 g of GelMA-30 or GelMA-60 solid (EFL, China) and 1 mL of initiator standard solution were added into the tube and heated in a water bath to dissolve completely. The GelMA solution was aspirated using a sterile syringe and filtered through a 0.22 µm sterile filter in an ultraclean table. The filtered sterile GelMA solution was irradiated with a 405 nm Ultraviolet (UV) light source for 30 s to solidify. The gelatinized samples were frozen at − 80 °C for 2 h, then dried in a vacuum dryer for 24 h. The samples were then sprayed with gold and placed on a scanning electron microscope (SEM; Gemini 2, Sigma, USA) irradiation stage for photography. Image J software was used to measure the average diameter of each hole and calculate the hole size based on the SEM photographs.

GelMA-exosomes distribution and release curve analysis

The 5% GelMA-30 was prepared according to the method mentioned above. BMSCs-exosomes were marked with PKH-26. An appropriate amount of BMSCs-exosomes was mixed with 5% GelMA-30 solution (the final concentration of exosomes was 50 µg/ml) and irradiated with UV light for 30 s to allow sufficient gelation. Subsequently, the distribution of BMSCs-exosomes in GelMA was observed by confocal microscopy. GelMA-exosomes was placed in 1 ml PBS. The supernatant was gathered daily and quantified after 7 days.

Establishment of rabbit TBJ injury model

All the animal experiments were approved by the Ethics Committee of Soochow University (Approval No.: SUDA20230619A02) and all animal manipulations were performed in accordance with the Guide for the Care and Use of Laboratory Animals of Soochow University. Additionally, the study was conducted in compliance with the ARRIVE guidelines.

A total of 72 three-month-old rabbits (weight 2.7 ± 0.2 kg) were studied. The rabbits were continuously anaesthetised using isoflurane inhalation anaesthesia. Successful anaesthesia was indicated by the disappearance of the corneal reflex. Surgical preparation of the left lower limb of the rabbit was treated. A longitudinal incision was made on the posterior lateral aspect of the lower leg using a blade to expose the flexor digitorum longus and tibia. Along the walk of the tendon, the flexor digitorum longus tendon was severed distally and the severed end was secured with suture. A 2.0 Kirschner wire (Pfizer, USA) was used to drill a hole in the lower 1/3 of the tibia vertically when fixed with a suture anchor (2.0 Mini Quickanchor Plus, AO, China) ($n=36$). A 4.0 Kirschner wire (Pfizer, USA) was used to drill when secured with an interference screw (5×12 mm Milagro BR Interference Screw, AO, China) ($n=36$) (Fig. 3). A 50 µg/ml GelMA-exosome mixture was prepared by encapsulating the exosomes in GelMA, which was subsequently injected into the TBJ site using a 1 ml syringe. Then, the experiment was divided equally into 3 groups according to the implants: (1) control group (only inject 1 ml PBS at the injury site), (2) GelMA group (only inject 1 ml GelMA at the injury site), (3) GelMA-exosomes group (inject 1 ml GelMA-exosomes at the injury site). The wound was then closed layer by layer and dressed with aseptic gauze. All animals resumed normal diets after the operation and were given ceftiofur sodium for

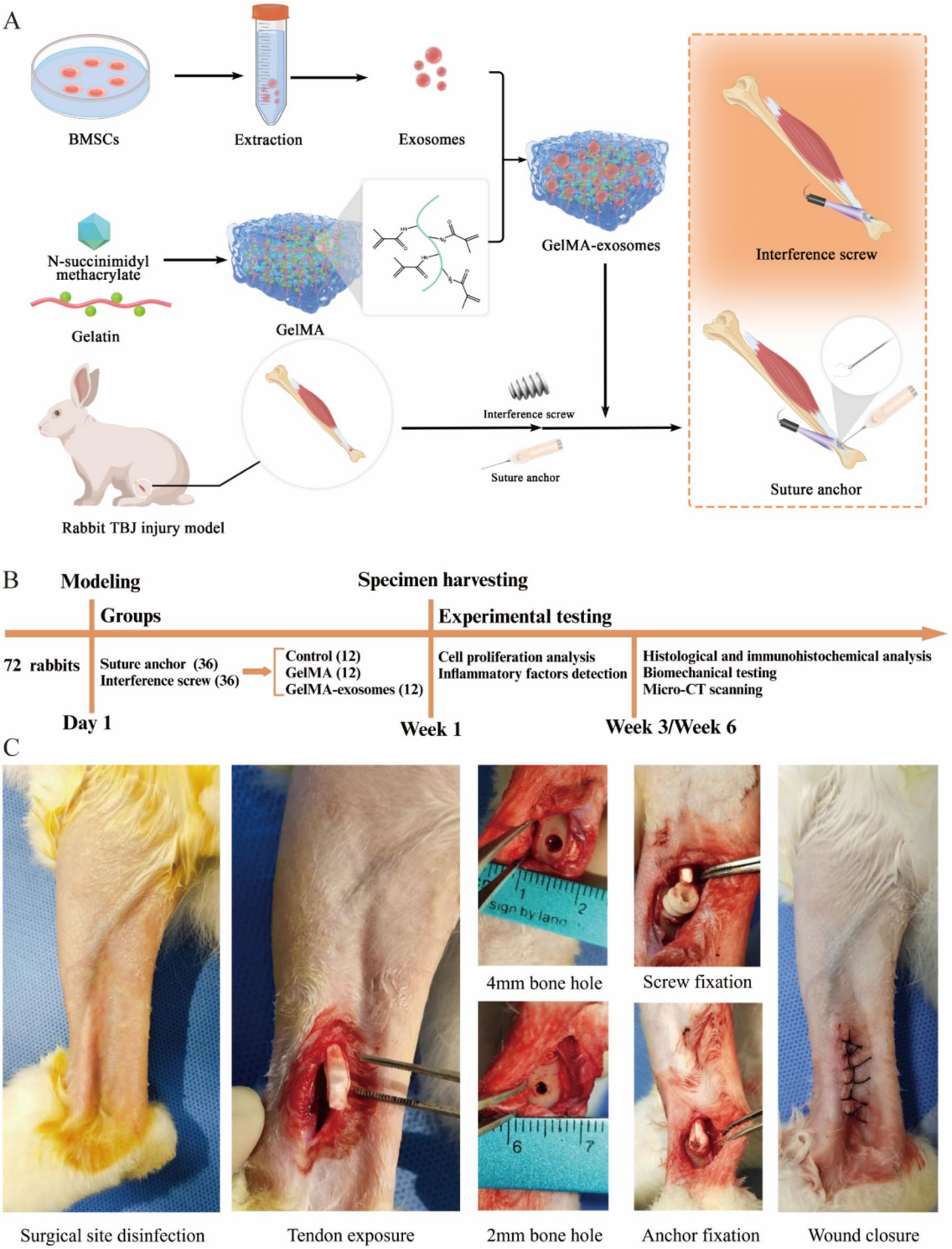

Fig. 3. The process of GelMA-exosomes preparation, the establishment of rabbit tendon-bone injury model and surgical treatment process. (**A**) Schematic diagram of the formation of GelMA-exosomes and their combination with an interference screw or suture anchor for the treatment of tendon-bone injuries in the rabbit model. (**B**) Flowchart of research design for animal experiments. (**C**)Surgical procedures in the rabbit model.

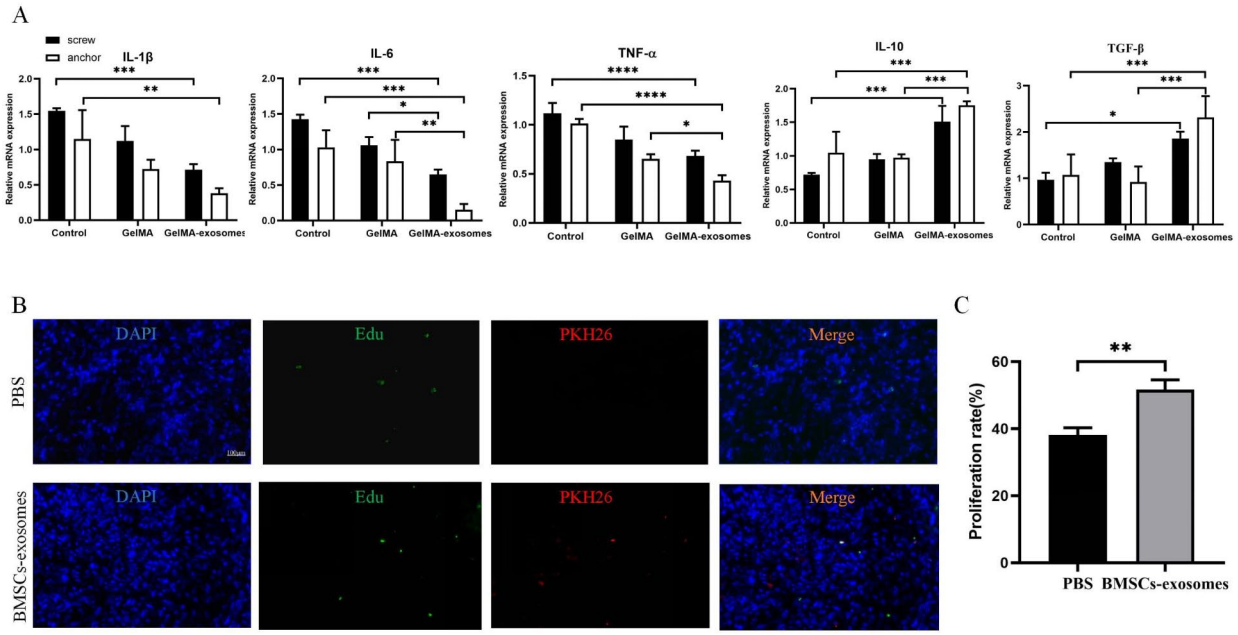

Fig. 4. BMSCs-exosomes could inhibit inflammatory factors and promote cell proliferation. (**A**) Relative expression of IL-1β, IL-6, TNF-α, IL-10, TGF-β genes at 7 days postoperatively. (**B**) In vivo detection of cell proliferation, the number of proliferating cells in the BMSCs-exosomes group were more than that in the PBS group, where the nuclei (DAPI staining in blue), proliferating cells (Edu staining in green), and exosomes (PKH-26 staining in red), Merge is the result of image superimposition. Scale bar: 100 μm. (**C**) Quantitative analysis of (**B**).

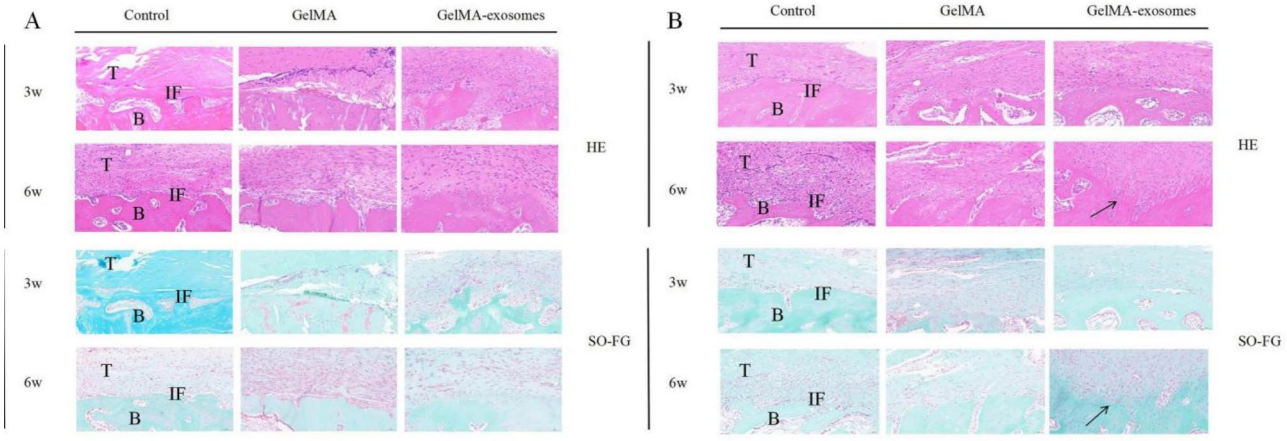

Fig. 5. Histological staining results. (**A**) HE, SO-FG staining images of specimens in the Control, GelMA and GelMA-exosomes groups at postoperative 3w and 6w after interference screw fixation. (**B**) HE, SO-FG staining images of specimens in the Control, GelMA and GelMA-exosomes groups at postoperative 3w and 6w after suture anchor fixation. T: tendon, B: bone, IF: interface. The black arrows show cartilage-like migratory structures. Scale bar: 50 μm.

anti-infection treatment the next day. The experimental animals were euthanised by intravenous pentobarbital. At 1 week postoperatively, qRT-PCR assays were performed to detect inflammatory factors at the TBJ and Edu assays were used to detect cell proliferation. HE staining, SO-FG staining, immunohistochemical analysis, Micro-CT analysis of surface bone volume changes, and biomechanical tests were used to detect the strength of tendon-bone healing at 3 and 6 weeks postoperatively.

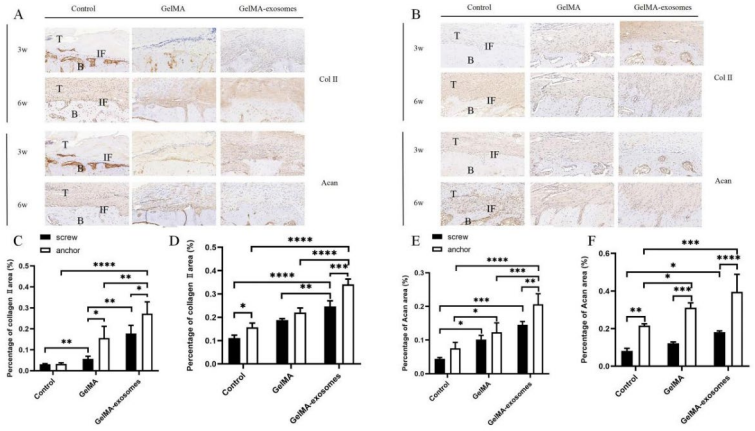

Fig. 6. Immunohistochemical staining and quantitative analysis results. (**A**) Col II and Acan immunohistochemical images of specimens in the Control, GelMA and GelMA-exosomes groups at 3w and 6w postoperatively during interference screw fixation. (**B**) Col II and Acan immunohistochemical images of specimens from Control, GelMA, and GelMA-exosomes groups at 3w and 6w postoperatively when fixed with suture anchors. T: tendon, B: bone, IF: interface. Scale bar: 50 μm. (**C**, **D**) Quantitative analysis of Col II immunohistochemistry in the Control, GelMA, and GelMA-exosomes groups at 3w and 6w with interference screw and suture anchor fixation. (**E**, **F**) Quantitative immunohistochemical analysis of Acan in the Control, GelMA, and GelMA-exosomes groups at 3w and 6w with interference screw and suture anchor fixation.

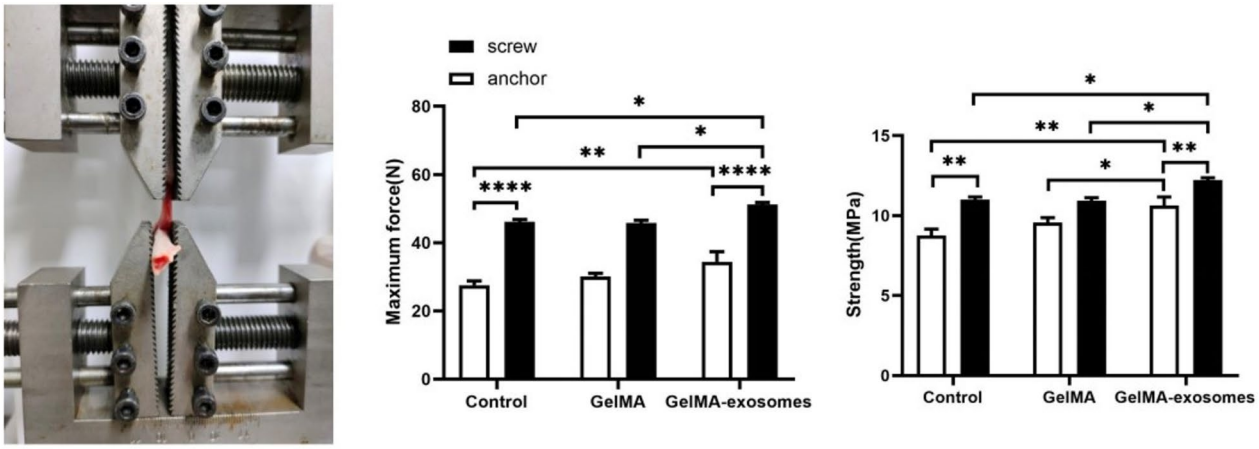

Fig. 7. Biomechanical testing of TBJ at 6 weeks after surgery. Maximum tensile force and strength analysis results of tendon-bone interface fixed with interference screw or suture anchor. Maximum tensile force was the maximum destructive force. Strength was obtained by dividing the maximum tensile force by the contact area of the TBJ.

qRT-PCR analysis

At one week after operation, animals of the corresponding group were sacrificed by air embolization introduced from the ear vein. The specimens from the TBJ were collected. 1 ml Trizol (Thermo Fisher, China) was added to the tissue and grinded. Subsequently, chloroform (Servicebio, China), isopropanol (Servicebio, China), and ethanol (Servicebio, China) were added in the appropriate proportions to extract the RNA. The primers were added according to the kit instructions (RiboBio, China) (Table 1), and performed the reverse transcription reaction at 42 °C for 60 min and 70 °C for 10 min. The cDNA concentration was measured after the reverse transcription. The reverse transcription products were amplified by adding the appropriate primers according to the kit instructions in a fluorescence PCR machine. The reaction program was set as follows: pre-denaturation at 95 °C for 10 min, denaturation at 95 °C for 2 s, annealing at 60 °C for 2 s, and extension at 70 °C for 10 s. A total of 40 cycles were performed. Melting curve analysis was performed immediately after the end of the cycle. CT values were obtained, and gene expression ploidy differences were calculated.

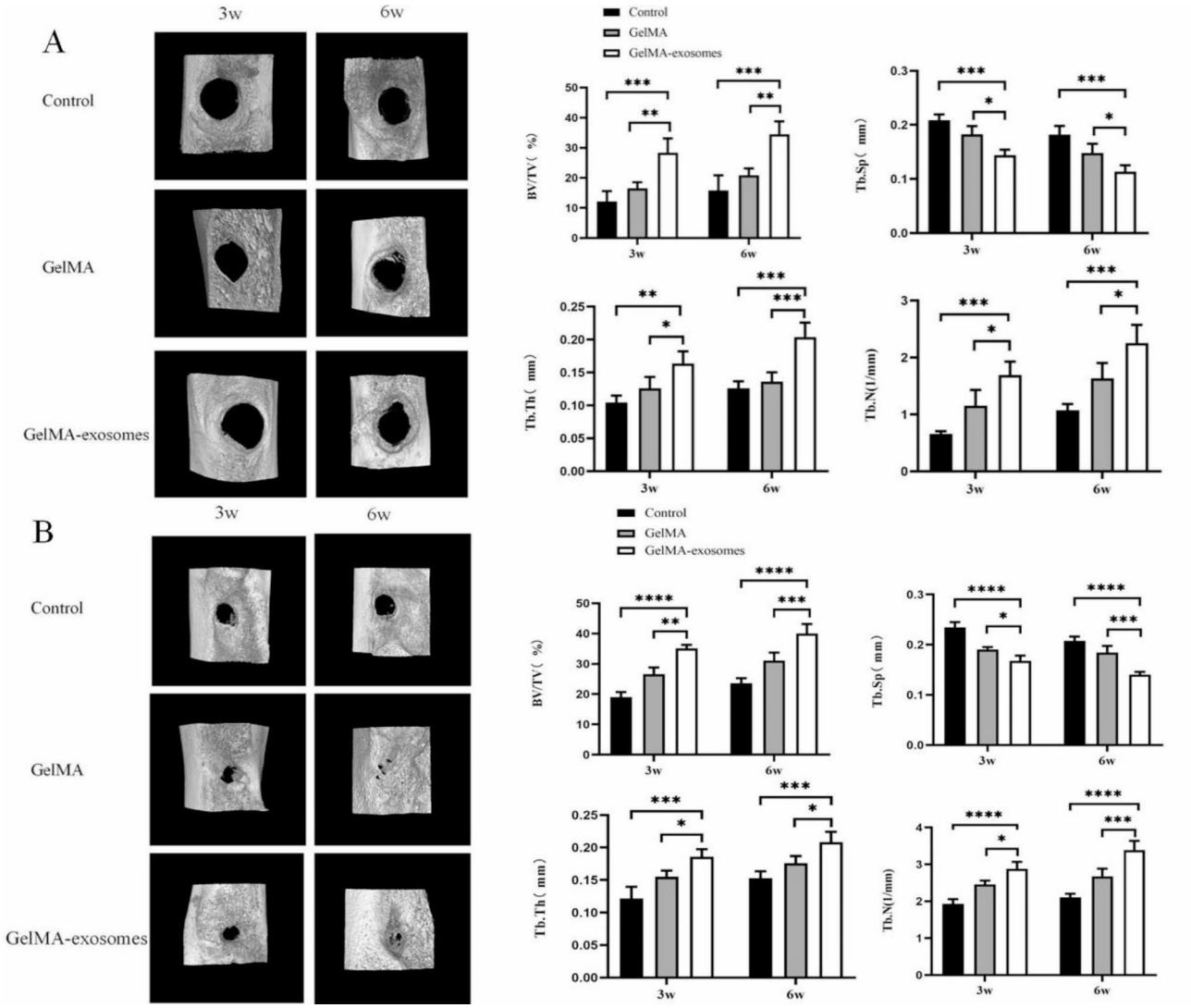

Fig. 8. The results of Micro-CT scanning. (**A**) 3D reconstruction of bone and quantitative analysis of BV/TV, Tb. Sp, Tb. Th and Tb. N during an interference screw fixation. (**B**) 3D reconstruction of bone and quantitative analysis of BV/TV, Tb. Sp, Tb. Th and Tb. N during a suture anchor fixation.

Gene name	Sequences
GAPDH	F:5'-ACTTTGTGAAGCTCATTTCCTGGTA-3'
	R:5'-GTGGTTTGAGGGCTCTTACTCCTT-3'
IL-1β	F:5'-TACAACAAGAGCTTCCGGCA-3'
	R:5'-GGCCACAGGTATCTTGTCGT-3'
IL-6	F:5'-GGCTGATAGAAGAAGACGGATG-3'
	R:5'-CCATGCCTGTCCAGAGATAAAG-3'
TNF-α	F:5'-CCTTCCTCTCCTCAGATGTTTC-3'
	R:5'-ACGGGTCAGTCACCAAATC-3'
IL-10	F:5'-TTGTTAACCGAGTCCCTGCT-3'
	R:5'-CCACTGCCTTGCTCTTGTTT-3'
TGF-β	F:5'-CAGTGGAAAGACCCCACATCTC-3'
	R:5'-GACGCAGGCAGCAATTATCC-3'

Table 1. Names of genes and sequences.

Cell proliferation analysis
Three days after surgery, 1 ml Edu staining solution (RiboBio, China) was injected subcutaneously. The corresponding rabbits were sacrificed after 4 days and specimens were collected from the TBJ. The specimens were collected for optimal cutting temperature compound (OCT, abcam) embedding to produce frozen sections, and 5 μm tissue sections were prepared. Staining was carried out according to the kit instructions (RiboBio, China), and 50 μl of anti-fluorescence quenching sealer was added to each specimen after staining was completed to seal the coverslips. Fluorescence microscopy (Nikon, China) was used for imaging and analysis.

Histological and immunohistochemical analysis
The specimens were fixed in 4% paraformaldehyde (Servicebio, China) for 24 h and decalcified in 15% EDTA (Servicebio, China) for 1 week. The fixed specimens were placed in tissue embedding boxes, and the serial numbers of the specimens were marked using an oil-based pen. The specimens were dehydrated in a gradient using different concentrations of ethanol, followed by wax immersion, embedding, and sectioning, with the thickness of the sections controlled at 3 μm. The sections were dehydrated in gradient alcohol at room temperature and stained for HE (Servicebio, China) and SO-FG (Servicebio, China). The corresponding anti-ACAN antibody (1:1000, Servicebio, China) and anti-Col II antibody (1:1000, Servicebio, China) were diluted at the corresponding ratios, and immunohistochemical staining was performed. The sections were stained and then air-dried. The sections were placed under a microscope for observation and image analysis.

Biomechanical testing
Specimens were collected 6 weeks after surgery and placed at − 80 °C for storage to prevent tissue damage. Samples were thawed at room temperature for more than 6 h before testing. The tendon tissue was fixed using a blood-repellent band to increase friction. Then, the specimen was fixed with clamps. The initial position of the tensiometer was adjusted so that the tester displays around 0 N. Then, the tensiometer was set to zero, and the tendon was stretched at a 5 mm/minute rate until the tendon-bone connection was separated. Measurements were taken to calculate the maximum tensile force and strength, where the maximum tensile force was the maximum rupture force, and strength was calculated by dividing the maximum tensile force by the contact area of the tendon-bone interface. The contact area for the interference screw group was calculated as follows: With a bone tunnel radius of 2 mm, the tendon-to-bone contact length is approximately one third of the tunnel's circumference, the depth is based on the cortical thickness of the tibia in rabbits, with a mean value of about 1 mm. Thus, the contact area is $1/3 \times \pi \times 2^2 \times 1 = 4\pi/3\ mm^2$. For the suture anchor group, the bone tunnel radius was 1 mm. The tendon was anchored at the tunnel's opening, making the contact area roughly the same as the area of the circular opening: $\pi \times 1^2 = \pi\ mm^2$.

Micro-CT scanning
The specimens were collected 3 and 6 weeks postoperatively and placed in 4% paraformaldehyde for 24 h of fixation. The specimens were then placed on a machine foam box and scanned after setting the scanning parameters. The X-ray scans were algorithmically reconstructed into tomograms using the NRecon Reconstruction software; the scanned tomograms were reconstructed in 3D using the CTVox software. CTan software was used to analyze the quality and density of new bone tissue within the bone tunnel and changes in bone quality around the bone tunnel.

Statistical analysis
This study used ImageJ software for image processing, SPSS 25.0 software for data analysis, and GraphPad Prism 8.0 software for plotting. Data between two groups were analyzed using an unpaired t-test, and differences between multiple groups were analyzed using ANOVA. T-tests were used to determine statistical differences between groups. Differences were considered statistically significant at $P < 0.05$ ($^{*}P < 0.05$, $^{**}P < 0.01$, $^{***}P < 0.001$, $^{****}P < 0.0001$).

Data availability
All data generated or analysed during this study are included in this published article.

Received: 30 March 2024; Accepted: 12 November 2024
Published online: 15 November 2024

References
1. Zelzer, E., Blitz, E., Killian, M. L. & Thomopoulos, S. Tendon-to-bone attachment: from development to maturity. *Birth Defects Res. C Embryo Today* **102**, 101–112. https://doi.org/10.1002/bdrc.21056 (2014).
2. Apostolakos, J. et al. The enthesis: a review of the tendon-to-bone insertion. *Muscles Ligaments Tendons J.* **4**, 333–342 (2014).
3. Yamamoto, M. et al. Development and regeneration of muscle, Tendon, and Myotendinous junctions in Striated skeletal muscle. *Int. J. Mol. Sci.* **23** https://doi.org/10.3390/ijms23063006 (2022).
4. Smith, L., Xia, Y., Galatz, L. M., Genin, G. M. & Thomopoulos, S. Tissue-engineering strategies for the tendon/ligament-to-bone insertion. *Connect. Tissue Res.* **53**, 95–105. https://doi.org/10.3109/03008207.2011.650804 (2012).
5. Shaw, H. M. & Benjamin, M. Structure-function relationships of entheses in relation to mechanical load and exercise. *Scand. J. Med. Sci. Sports* **17**, 303–315. https://doi.org/10.1111/j.1600-0838.2007.00689.x (2007).
6. Thomopoulos, S., Williams, G. R., Gimbel, J. A., Favata, M. & Soslowsky, L. J. Variation of biomechanical, structural, and compositional properties along the tendon to bone insertion site. *J. Orthop. Res.* **21**, 413–419. https://doi.org/10.1016/s0736-0266(03)00057-3 (2003).
7. Villegas, D. F., Maes, J. A., Magee, S. D. & Donahue, T. L. Failure properties and strain distribution analysis of meniscal attachments. *J. Biomech.* **40**, 2655–2662. https://doi.org/10.1016/j.jbiomech.2007.01.015 (2007).

8. Stouffer, D. C., Butler, D. L. & Hosny, D. The relationship between crimp pattern and mechanical response of human patellar tendon-bone units. *J. Biomech. Eng.* **107**, 158–165. https://doi.org/10.1115/1.3138536 (1985).
9. Shi, Y. et al. Exosomes Derived from Bone Marrow Stromal cells (BMSCs) enhance Tendon-Bone Healing by regulating macrophage polarization. *Med. Sci. Monit.* **26**, e923328. https://doi.org/10.12659/msm.923328 (2020).
10. Andrzejewska, A., Lukomska, B. & Janowski, M. Concise Review: mesenchymal stem cells: from roots to Boost. *Stem Cells* **37**, 855–864. https://doi.org/10.1002/stem.3016 (2019).
11. Caplan, A. I. Mesenchymal stem cells. *J. Orthop. Res.* **9**, 641–650. https://doi.org/10.1002/jor.1100090504 (1991).
12. Cai, H. & Guo, H. Mesenchymal stem cells and their exocytotic vesicles. *Int. J. Mol. Sci.* **24** https://doi.org/10.3390/ijms24032085 (2023).
13. Lu, J. et al. Tendon-to-bone Healing in a rat extra-articular bone tunnel model: a comparison of fresh autologous bone marrow and bone marrow-derived mesenchymal stem cells. *Am. J. Sports Med.* **47**, 2729–2736. https://doi.org/10.1177/0363546519862284 (2019).
14. Tang, Y. et al. Structure and ingredient-based biomimetic scaffolds combining with autologous bone marrow-derived mesenchymal stem cell sheets for bone-tendon healing. *Biomaterials* **241**, 119837. https://doi.org/10.1016/j.biomaterials.2020.119837 (2020).
15. Jiang, L. et al. Mesenchymal stem cells: an efficient cell therapy for tendon repair (review). *Int. J. Mol. Med.* **52** https://doi.org/10.3892/ijmm.2023.5273 (2023).
16. Lui, P. P. Y. & Leung, Y. T. Practical considerations for translating mesenchymal stromal cell-derived extracellular vesicles from bench to Bed. *Pharmaceutics* **2022**, 14. https://doi.org/10.3390/pharmaceutics14081684 (2022).
17. Maruyama, M. et al. The effect of mesenchymal stem cell sheets on early healing of the achilles tendon in rats. *Tissue Eng. Part. A* **26**, 206–213. https://doi.org/10.1089/ten.TEA.2019.0163 (2020).
18. Shi, Z., Wang, Q. & Jiang, D. Extracellular vesicles from bone marrow-derived multipotent mesenchymal stromal cells regulate inflammation and enhance tendon healing. *J. Transl. Med.* **17**, 211. https://doi.org/10.1186/s12967-019-1960-x (2019).
19. Koch, D. W., Schnabel, L. V., Ellis, I. M., Bates, R. E. & Berglund, A. K. TGF-β2 enhances expression of equine bone marrow-derived mesenchymal stem cell paracrine factors with known associations to tendon healing. *Stem Cell. Res. Ther.* **13**, 477. https://doi.org/10.1186/s13287-022-03172-9 (2022).
20. Xitong, D. & Xiaorong, Z. Targeted therapeutic delivery using engineered exosomes and its applications in cardiovascular diseases. *Gene* **575**, 377–384. https://doi.org/10.1016/j.gene.2015.08.067 (2016).
21. Kalluri, R. & LeBleu, V. S. The biology, function, and biomedical applications of exosomes. *Science*. **367** https://doi.org/10.1126/science.aau6977 (2020).
22. Hade, M. D., Suire, C. N. & Suo, Z. Mesenchymal stem cell-derived exosomes: applications in regenerative medicine. *Cells* **10**, 526. https://doi.org/10.3390/cells10081959 (2021).
23. Han, L. et al. Exosome-delivered BMP-2 and polyaspartic acid promotes tendon bone healing in rotator cuff tear via Smad/RUNX2 signaling pathway. *Bioengineered* **13**, 1459–1475. https://doi.org/10.1080/21655979.2021.2019871 (2022).
24. Huang, Y. et al. Bone marrow mesenchymal stem cell-derived exosomes promote rotator cuff tendon-bone healing by promoting angiogenesis and regulating M1 macrophages in rats. *Stem Cell. Res. Ther.* **11**, 496. https://doi.org/10.1186/s13287-020-02005-x (2020).
25. He, S. et al. Arthritic microenvironment-dictated fate decisions for stem cells in cartilage repair. *Adv. Sci. (Weinh)* **10**, e2207715. https://doi.org/10.1002/advs.202207715 (2023).
26. Chen, P. et al. Desktop-stereolithography 3D printing of a radially oriented extracellular matrix/mesenchymal stem cell exosome bioink for osteochondral defect regeneration. *Theranostics* **9**, 2439–2459. https://doi.org/10.7150/thno.31017 (2019).
27. Ju, Y., Hu, Y., Yang, P., Xie, X. & Fang, B. Extracellular vesicle-loaded hydrogels for tissue repair and regeneration. *Mater. Today Bio.* **18**, 100522. https://doi.org/10.1016/j.mtbio.2022.100522 (2023).
28. Su, C. A. et al. Femoral interference screw fixation in ACL Reconstruction using Bone-Patellar Tendon-Bone Grafts. *JBJS Rev.* **8**, e0066. https://doi.org/10.2106/jbjs.Rvw.19.00066 (2020).
29. Kim, J. G. et al. Enhancement of tendon-bone healing with the use of bone morphogenetic protein-2 inserted into the suture anchor hole in a rabbit patellar tendon model. *Cytotherapy* **16**, 857–867. https://doi.org/10.1016/j.jcyt.2013.12.012 (2014).
30. Sequeira, S. B., Imbergamo, C. & Gould, H. P. Interference screws are biomechanically superior to suture anchors for medial patellofemoral ligament reconstruction: a systematic review and meta-analysis. *Arthrosc. Sports Med. Rehabil* **4**, e1581–e1588. https://doi.org/10.1016/j.asmr.2022.05.003 (2022).
31. Migliorini, F., Baroncini, A., Eschweiler, J., Tingart, M. & Maffulli, N. Interference screws vs. suture anchors for isolated medial patellofemoral ligament femoral fixation: a systematic review. *J. Sport Health Sci.* **11**, 123–129. https://doi.org/10.1016/j.jshs.2020.11.011 (2022).
32. Xu, B., Yin, Y., Zhu, Y., Yin, Y. & Fu, W. Comparison of bioabsorbable and metallic interference screws for graft fixation during ACL reconstruction: a meta-analysis of randomized controlled trials. *Orthop. J. Sports Med.* **9**, 23259671211021577. https://doi.org/10.1177/23259671211021577 (2021).
33. Ntalos, D. et al. All-suture anchor pullout results in decreased bone damage and depends on cortical thickness. *Knee Surg. Sports Traumatol. Arthrosc.* **29**, 2212–2219. https://doi.org/10.1007/s00167-020-06004-6 (2021).
34. Pei, Z. et al. Experimental study on repair of cartilage defects in the rabbits with GelMA-MSCs scaffold prepared by three-dimensional bioprinting. *Int. J. Bioprint* **9**, 662. https://doi.org/10.18063/ijb.v9i2.662 (2023).
35. Kawamura, S., Ying, L., Kim, H. J., Dynybil, C. & Rodeo, S. A. Macrophages accumulate in the early phase of tendon-bone healing. *J. Orthop. Res.* **23**, 1425–1432. https://doi.org/10.1016/j.orthres.2005.01.014.1100230627 (2005).
36. Li, Z. et al. BMSC-derived exosomes promote tendon-bone healing after anterior cruciate ligament reconstruction by regulating M1/M2 macrophage polarization in rats. *Stem Cell. Res. Ther.* **13**, 295. https://doi.org/10.1186/s13287-022-02975-0 (2022).
37. Wang, J. et al. Synergistic therapy of Celecoxib-loaded magnetism-responsive hydrogel for Tendon tissue injuries. *Front. Bioeng. Biotechnol.* **8**, 592068. https://doi.org/10.3389/fbioe.2020.592068 (2020).
38. Gögele, C., Hahn, J. & Schulze-Tanzil, G. Anatomical tissue engineering of the anterior cruciate ligament entheses. *Int. J. Mol. Sci.* **24** https://doi.org/10.3390/ijms24119745 (2023).
39. Luo, Z. et al. Mechano growth factor (MGF) and transforming growth factor (TGF)-β3 functionalized silk scaffolds enhance articular hyaline cartilage regeneration in rabbit model. *Biomaterials* **52**, 463–475. https://doi.org/10.1016/j.biomaterials.2015.01.001 (2015).
40. Kovacevic, D. et al. Calcium-phosphate matrix with or without TGF-β3 improves tendon-bone healing after rotator cuff repair. *Am. J. Sports Med.* **39**, 811–819. https://doi.org/10.1177/0363546511399378 (2011).
41. Chen, W. et al. Conditioned medium of human bone marrow-derived stem cells promotes tendon-bone healing of the rotator cuff in a rat model. *Biomaterials* **271**, 120714. https://doi.org/10.1016/j.biomaterials.2021.120714 (2021).
42. Xu, Y. et al. Stem cell therapies in tendon-bone healing. *World J. Stem Cells* **13**, 753–775. https://doi.org/10.4252/wjsc.v13.i7.753 (2021).
43. Røsland, G. V. et al. Long-term cultures of bone marrow-derived human mesenchymal stem cells frequently undergo spontaneous malignant transformation. *Cancer Res.* **69**, 5331–5339. https://doi.org/10.1158/0008-5472.Can-08-4630 (2009).
44. Shen, H. et al. The effect of mesenchymal stromal cell sheets on the inflammatory stage of flexor tendon healing. *Stem Cell. Res. Ther.* **7**, 144. https://doi.org/10.1186/s13287-016-0406-0 (2016).
45. Ferguson, S. W. et al. The microRNA regulatory landscape of MSC-derived exosomes: a systems view. *Sci. Rep.* **8**, 1419. https://doi.org/10.1038/s41598-018-19581-x (2018).

46. Yu, H. et al. Bone marrow mesenchymal stem cell-derived exosomes promote tendon regeneration by facilitating the proliferation and migration of endogenous tendon stem/progenitor cells. *Acta Biomater.* **106**, 328–341. https://doi.org/10.1016/j.actbio.2020.01.051 (2020).
47. Liu, H. et al. Adipose-derived mesenchymal stromal cell-derived exosomes promote tendon healing by activating both SMAD1/5/9 and SMAD2/3. *Stem Cell. Res. Ther.* **12**, 338. https://doi.org/10.1186/s13287-021-02410-w (2021).
48. Zou, J. et al. Therapeutic potential and mechanisms of mesenchymal stem cell-derived exosomes as bioactive materials in tendon-bone healing. *J. Nanobiotechnol.* **21**, 14. https://doi.org/10.1186/s12951-023-01778-6 (2023).
49. Cao, Y. et al. Three-dimensional printed multiphasic scaffolds with stratified cell-laden gelatin methacrylate hydrogels for biomimetic tendon-to-bone interface engineering. *J. Orthop. Translat* **23**, 89–100. https://doi.org/10.1016/j.jot.2020.01.004 (2020).
50. Huang, B., Yang, M., Kou, Y. & Jiang, B. Absorbable implants in sport medicine and arthroscopic surgery: a narrative review of recent development. *Bioact Mater.* **31**, 272–283. https://doi.org/10.1016/j.bioactmat.2023.08.015 (2024).
51. Milano, G. et al. Comparison between different femoral fixation devices for ACL reconstruction with doubled hamstring tendon graft: a biomechanical analysis. *Arthroscopy* **22**, 660–668. https://doi.org/10.1016/j.arthro.2006.04.082 (2006).
52. Kahlon, H. et al. Surgical techniques for medial patellofemoral ligament reconstruction: a systematic review and meta-analysis of level I and II studies. *Knee Surg. Sports Traumatol. Arthrosc.* **31**, 4368–4378. https://doi.org/10.1007/s00167-023-07494-w (2023).
53. Gao, H. et al. Regulating macrophages through Immunomodulatory Biomaterials is a Promising Strategy for promoting Tendon-Bone Healing. *J. Funct. Biomater.* **13**, 859. https://doi.org/10.3390/jfb13040243 (2022).

Acknowledgements

This work was supported by the Priority Academic Program Development of Jiangsu Higher Education Institutions (PAPD) and Health and Family Planning Commission Research Project of Jiangsu Province (H201619).

Author contributions

M.G.: Conceptualization, Investigation, Formal analysis, Writing – original draft, Writing – review & editing. P.Z.: Methodology, Investigation, Software, Validation, Writing – review & editing. J.X.: Formal analysis. Z.W.: Investigation. Y.X.: Visualization. Y.Y.: Data collection. H.Z.: Data curation, Funding acquisition, Project administration, Supervision. J.Q.: Conceptualization, Methodology, Funding acquisition, Writing – review & editing.

Competing interests

The authors declare no competing interests.

Additional information

Supplementary Information The online version contains supplementary material available at https://doi.org/10.1038/s41598-024-79787-0.

Correspondence and requests for materials should be addressed to H.Z. or J.Q.